International Journal of Mathematical Archive-2(11), 2011, Page: 2229-2240
Available online through www.ijma.info ISSN 2229 – 5046

EFFECT OF VISCOUS DISSIPATION ON MHD FLOW AND HEAT TRANSFER OF A DUSTY FLUID OVER AN UNSTEADY STRETCHING SHEET

G. S. Roopa, B. J. Gireesha*[1] and C. S. Bagewadi

[1]Department of Studies and Research in Mathematics, Kuvempu University, Shankaraghatta-577 451, Shimoga, Karnataka, INDIA

**E-mail: bjgireesu@rediffmail.com*

(Received on: 10-11-11; Accepted on: 24-11-11)

ABSTRACT

This paper is focused on the study of hydromagnetic boundary layer flow and heat transfer of a viscous, incompressible, dusty fluid over a stretching sheet with the effect of viscous dissipation. The equations of motion and heat transfer are reduced to system of coupled non-linear ordinary differential equations using similarity transformations. These non-linear differential equations are solved numerically by using RKF-45 method. The two different cases of heating process are studied, namely, (i) a sheet with variable wall temperature (VWT case) and (ii) a sheet with variable heat flux (VHF case). The effects of the various parameters entering into the problem on the velocity fields and temperature distributions are discussed both in graphical and tabular form. Comparisons of numerical results were made with previously published results.

Key Words: *Boundary layer flow, heat transfer, stretching sheet, dusty fluid, viscous dissipation, numerical solution.*

AMS Subject Classification (2000): *76T15, 80A20;*

1. INTRODUCTION:

The study of two-dimensional boundary layer flow and heat transfer of a dusty fluid over a stretching sheet has gained much interest in recent times because of its numerous industrial applications like polymer processing of a chemical engineering plant and in metallurgy for the metal processing. Few examples of such technological processes are the cooling of an infinite metallic plate in a cooling bath, the boundary layer along material handling conveyers, the boundary layer along a liquid film in condensation processes. It is also encountered in other process like annealing and tinning of copper wires, continuous casting, spinning of fibers, and the aerodynamic extrusion of plastic sheets, crystal growing, drawing plastic films, the cooling or drying of papers, glass blowing and so on. In these cases, the quality of the final product depends on the rate of heat transfer at the stretching surface. The problem of flow due to a stretching sheet has been later extended too many flow situations.

Sakiadis [14, 15] initiated the study of boundary layer flow over a continuous solid surface moving with constant speed. Crane [6] studied the boundary layer flow of a Newtonian fluid caused by the stretching of an elastic flat surface and presented exact solutions. Datta et al. [7] have investigated boundary layer flow of a dusty fluid over a semi-infinite flat plate. Grubka et al. [13] carried out heat transfer studies by considering the power law variation of surface temperature. Vajravelu et al. [19] studied hydromagnetic flow of a dusty fluid over a stretching sheet including, the effects of suction. The effects of buoyancy force on the development of velocity and thermal boundary layer flows over a stretching sheet has been initiated by Chen [3]. Elbashbeshy et al. [9] studied the heat transfer over an unsteady stretching surface.

Cortell [5] analyzed the flow of an electrically conducting power-law fluid in the presence of a uniform transverse magnetic field over a stretching sheet. Sharidan et al. [17] obtained the similarity solutions for the unsteady boundary layer flow and heat transfer over a stretching sheet for special distributions of the stretching velocity and surface temperature. Aziz [1] obtained the numerical solution for laminar thermal boundary over a flat plate with a convective surface boundary condition using the symbolic algebra software Maple. The problem of magneto-hydrodynamic mixed convective flow and heat transfer of an electrically conducting, power-law fluid past a stretching surface in the presence of heat generation/absorption and thermal radiation has been analyzed by Chen [4]. Dulal et al. [8] have studied hydromagnetic non-Darcy flow and heat transfer over a stretching sheet in the presence of thermal radiation and

Corresponding author: B. J. Gireesha*,*E-mail: bjgireesu@rediffmail.com

Ohmic dissipation. Anjali et al. [2] presented the study of dissipation effects on MHD nonlinear flow and heat transfer past a porous surface with prescribed heat flux.

The study of magnetohydrodynamic flows with viscous dissipation has many important industrial, technological and geothermal applications such as high temperature plasmas, cooling of nuclear reactors, liquid metal fluids, MHD accelerators and power generation systems. The analytical results were carry out by Vajravelu et al. [18] who took into account the effects of viscous dissipation and internal heat generation. Veena et al. [20] have obtained the solution of heat transfer in a visco-elastic fluid past a stretching sheet with viscous dissipation and internal heat generation. Recently Gireesha et al. [10, 12] studied unsteady hydromagnetic boundary layer flow and heat transfer of dusty fluid over a stretching sheet. Further, they [11] studied boundary layer flow and heat transfer of a dusty fluid flow over a stretching sheet with non-uniform heat source/sink.

In this analysis, the MHD boundary layer flow and heat transfer of a dusty fluid over a stretching sheet in an incompressible fluid with the effect of viscous dissipation is considered. The coupled non-linear partial differential equations governing the problem are reduced to a system of coupled non-linear ordinary differential equations by applying suitable similarity transformations. The system of equations is then solved by employing Runge-Kutta-Fehlberg-45 method with the help of Maple software. Numerical results of the local skin friction coefficient and the local Nusselt number as well as the velocity and the temperature profiles are examined for different physical parameters both in graphical and tabular form.

2. FLOW ANALYSIS OF THE PROBLEM:

Consider an unsteady, two-dimensional laminar boundary layer flow and heat transfer of an incompressible, viscous dusty fluid over a continuous moving stretching sheet. The x-axis is taken along the stretching surface in the direction of the motion with the slot as the origin, and the y-axis is perpendicular to the sheet in the outward direction towards the fluid. The flow is assumed to be confined in a region $y > 0$. The flow is caused by the stretching of the sheet that moves in its own plane with the surface velocity $U_w(x,t)$. It is considered that the wall temperature $T_w(x,t)$ of the sheet is suddenly raised from T_∞ to $T_w(x,t)\ (> T_\infty)$ or there is suddenly imposed a heat flux $q_w(x,t)$ at the wall. Further, viscous dissipation term is retained in the energy equation. Under these assumptions, the boundary layer form of the governing boundary layer equations can be written as

$$\frac{\partial u}{\partial x}+\frac{\partial v}{\partial y}=0, \tag{1}$$

$$\frac{\partial u}{\partial t}+u\frac{\partial u}{\partial x}+v\frac{\partial v}{\partial y}=\frac{\mu}{\rho}\frac{\partial^2 u}{\partial y^2}+\frac{kN}{\rho}\left(u_p-u\right)-\frac{\sigma\hat{B}_0^2}{\rho}u, \tag{2}$$

$$\frac{\partial u_p}{\partial t}+u_p\frac{\partial u_p}{\partial x}+v_p\frac{\partial u_p}{\partial y}=\frac{k}{m}(u-u_p) \tag{3}$$

$$\frac{\partial v_p}{\partial t}+u_p\frac{\partial v_p}{\partial x}+v_p\frac{\partial v_p}{\partial y}=\frac{k}{m}(v-v_p) \tag{4}$$

$$\frac{\partial(Nu_p)}{\partial x}+\frac{\partial(Nv_p)}{\partial y}=0, \tag{5}$$

where x and y represents coordinate axes along the continuous surface in the direction of motion and perpendicular to it, respectively, (u,v) and (u_p,v_p) denote the velocity components of the fluid and particles along the x and y directions respectively, t is the time, $\mu,\rho,\sigma,\hat{B}_0$ and k are the coefficient of viscosity of fluid, density of the fluid, electrical conductivity, induced magnetic field and Stoke's resistance co-efficient respectively, m and N are the mass concentration and number density of the particle phase. In deriving these equations, the Stokesian drag force is considered for the interaction between the fluid and particle phase. Also, it is assumed that the external electric field is zero and the electric field due to polarization of charges is negligible.

In order to solve the governing boundary layer equations consider the following appropriate boundary conditions on velocity:

$$u=U_w(x,t),\ v=V_w(x,t)\ \text{ at }\ y=0,$$

$$u\to 0,\ u_p\to 0,\ v_p\to v,\ N\to\rho E\ \text{ as }\ y\to\infty, \tag{6}$$

where $U_w = \frac{bx}{1-at}$ is the sheet velocity, b is the initial stretching rate being a positive constant, a is positive constant which measures the unsteadiness, whereas the effective stretching rate $b/(1-at)$ is increasing with time since $a > 0$, $V_w(x,t) = -\frac{v_0}{\sqrt{1-at}}$ is the suction velocity and E is the density ratio.

Equations (1)-(5), when subjected to boundary condition (6), admits self-similar solutions in terms of the similarity function f and similarity variable η as

$$u = \frac{bx}{1-at} f'(\eta), \quad v = -\sqrt{\frac{b\nu}{(1-at)}} f(\eta), \quad \eta = \sqrt{\frac{b}{\nu(1-at)}}\, y,$$

$$u_p = \frac{bx}{1-at} F(\eta), \quad v_p = \sqrt{\frac{b\nu}{(1-at)}} G(\eta), \quad \rho_r = H(\eta), \quad \hat{B}_0 = B_0(1-at)^{-1/2} \tag{7}$$

These equations identically satisfy the governing equation (1). Substitute (7) into the (2)-(5), then one can get

$$f'''(\eta) + f(\eta)f''(\eta) - f'(\eta)^2 - \alpha\left[f'(\eta) + \frac{\eta}{2} f''(\eta)\right] + l\beta H(\eta)[F(\eta) - f'(\eta)] - Mf'(\eta) = 0, \tag{8}$$

$$G(\eta)F'(\eta) + F(\eta)^2 - \beta[f'(\eta) - F(\eta)] + \alpha\left[F(\eta) + \frac{\eta}{2}F'(\eta)\right] = 0, \tag{9}$$

$$G(\eta)G'(\eta) + \beta[f(\eta + G(\eta)] + \frac{\alpha}{2}[G(\eta) + \eta G'(\eta)] = 0, \tag{10}$$

$$F(\eta)H(\eta) + G'(\eta)H(\eta) + H'(\eta)G(\eta) = 0, \tag{11}$$

where a prime denotes the differentiation with respect to η and $l = \frac{mN}{\rho}$ is the mass concentration, $\beta = \frac{1}{\tau b}(1-at)$ is the fluid-particle interaction parameter, $\alpha = \frac{a}{b}$ is a parameter that measures the unsteadiness, $\rho_r = \frac{N}{\rho}$ is the relative density, $M = \frac{\sigma B_0^2}{\rho b}$ is the magnetic field parameter.

Similarity boundary conditions (6) will become

$$f'(\eta) = 1, \quad f(\eta) = f_0 \quad \text{at} \quad \eta = 0,$$

$$f'(\eta) = 0, \quad F(\eta) = 0, \quad G(\eta) = -f(\eta), \quad H(\eta) = E \quad \text{as} \quad \eta \to \infty. \tag{12}$$

where $f_0 = \frac{v_0}{\sqrt{b\nu}}$, $f_0 > 0$ is a suction parameter.

3. HEAT TRANSFER ANALYSIS:

The governing unsteady, dusty boundary layer heat transport equations with thermal conductivity and viscous dissipation are given by

$$\rho c_p\left[\frac{\partial T}{\partial t} + u\frac{\partial T}{\partial x} + v\frac{\partial T}{\partial y}\right] = k^*\frac{\partial^2 T}{\partial y^2} + \frac{Nc_p}{\tau_T}(T_p - T) + \frac{N}{\tau_v}(u_p - u)^2 + \frac{\mu}{\rho c_p}\left(\frac{\partial u}{\partial y}\right)^2, \tag{13}$$

$$Nc_m\left[\frac{\partial T_p}{\partial t} + u_p\frac{\partial T_p}{\partial x} + v_p\frac{\partial T_p}{\partial y}\right] = -\frac{Nc_p}{\tau_T}(T_p - T), \tag{14}$$

where T and T_p are the temperatures of the fluid and dust particle inside the boundary layer, c_p and c_m are the specific heat of fluid and dust particles, τ_T is the thermal equilibrium time and is time required by the dust cloud to adjust its temperature to the fluid, k^* is the thermal conductivity, τ_v is the relaxation time of the of dust particle i.e., the time required by a dust particle to adjust its velocity relative to the fluid.

To solve the temperature equations (13) and (14), we consider two general cases of temperature boundary conditions, namely

(1) Boundary with variable wall temperature (VWT) and

(2) Boundary with variable heat flux (VHF).

CASE-1: Variable Wall Temperature (VWT-Case):

For this heating process, employ the following variable wall temperature boundary conditions:

$$T = T_w(x,t) \quad \text{at} \quad y = 0,$$

$$T \to T_\infty, \qquad T_p \to T_\infty \quad \text{as} \quad y \to \infty, \tag{15}$$

where $T_w = T_\infty + T_0\left[\frac{bx^2}{\nu(1-at)^2}\right]$ is the surface temperature of the sheet varies with the distance x from the slot and time t, T_0 is a reference temperature such $0 \le T_0 \le T_w$ and T_∞ is the temperature far away from the stretching surface with $T_W > T_\infty$.

Introduce the dimensionless variables for the temperatures $\theta(\eta)$ and $\theta_p(\eta)$ as follows:

$$\theta\,(\eta) = \frac{T-T_\infty}{T_w-T_\infty}, \qquad \theta_p(\eta) = \frac{T_p-T_\infty}{T_w-T_\infty}, \tag{16}$$

where $\mathrm{T}-T_\infty = T_0\left[\frac{bx^2}{\nu(1-at)^2}\right]\theta(\eta)$.

Using the similarity variable η and (16) into (13) and (14), one can arrive the following dimensionless system of equations:

$$\theta''(\eta) + \mathrm{Pr}[f(\eta)\theta'(\eta) - 2f'(\eta)\theta(\eta)] + \frac{Nc_1}{\rho}Pr[\theta_p(\eta) - \theta(\eta)]$$
$$+c_2 NPrEc[F(\eta) - f'(\eta)]^2 - \frac{\alpha}{2}\mathrm{Pr}[4\theta(\eta) + \eta\theta'(\eta)] + \mathrm{Pr}\,Ec\,[f''(\eta)]^2 = 0,, \tag{17}$$

$$G(\eta)\theta_p'(\eta) + 2F(\eta)\theta_p(\eta) + \frac{\alpha}{2}\left[4\theta_p(\eta) + \eta\theta_p'(\eta)\right] + \gamma c_1\left[\theta_p(\eta) - \theta(\eta)\right] = 0, \tag{18}$$

where $Pr = \mu c_p/k^*$ is Prandtl number, $c_1 = (1-at)/\tau_T b$ is the local fluid-particle interaction parameters for temperature, $\gamma = c_p/c_m$, $c_2 = (1-at)/\mu\tau_v$ is the local fluid-particle interaction parameter of velocity and $Ec = U_w^2/C_p(T_w - T_\infty)$ is the local Eckert number.

Corresponding thermal boundary conditions for $\theta(\eta)$ and $\theta_p(\eta)$ as

$$\theta(\eta) = 1 \quad \text{at} \quad \eta = 0,$$

$$\theta(\eta) = 0, \quad \theta_p(\eta) = 0 \quad \text{as} \quad \eta \to \infty. \tag{19}$$

CASE-2: Variable Heat Flux (VHF-Case):

In VHF case, define the following boundary conditions on temperature as follows:

$$\frac{\partial T}{\partial y} = -\frac{q_w(x,t)}{k} \quad \text{at} \quad y = 0,$$

$$T \to T_\infty, \qquad T_p \to T_\infty \quad \text{as} \quad y \to \infty, \tag{20}$$

where $q_w(x,t) = q_{w_0}\,x^2\left(\frac{b}{\nu}\right)^{3/2}(1-at)^{-5/2}$.

In order to obtain similarity solution for temperature, define dimensionless temperature variables in VHF case as in equation (16) where $\mathrm{T}= T_\infty + \frac{q_{w_0}}{k}\left[\frac{bx^2}{\nu(1-at)^2}\right]g(\eta)$. With the help of these in equations (13) and (14), one can get the following non-dimensional equations in terms of $g(\eta)$ and $g_p(\eta)$ as

$$\theta''(\eta)+\Pr[f(\eta)\theta'(\eta)-2f'(\eta)\theta(\eta)]+\frac{Nc_1}{\rho}Pr[\theta_p(\eta)-\theta(\eta)+c_2NPrEc[F(\eta)-f'(\eta)]^2$$
$$-\frac{\alpha}{2}\Pr[4\theta(\eta)+\eta\theta'(\eta)]+\Pr Ec\,[f''(\eta)]^2=0, \tag{21}$$

$$G(\eta)\theta_p'(\eta)+2F(\eta)\theta_p(\eta)+\frac{\alpha}{2}\left[4\theta_p(\eta)+\eta\theta_p'(\eta)\right]++\gamma c_1\left[\theta_p(\eta)-\theta(\eta)\right]=0, \tag{22}$$

The corresponding boundary conditions will get the following form

$$\theta'(\eta)=-1 \quad \text{at} \quad \eta=0,$$
$$\theta(\eta)=0, \quad \theta_p(\eta)=0 \quad \text{as} \quad \eta\to\infty. \tag{23}$$

The physical quantities of interest in this problem are the skin friction coefficient c_f and the local Nusselt number Nu_x, which are defined as

$$c_f=\frac{\tau_w}{\rho U_w^2}, \quad Nu_x=\frac{xq_w}{k^*(T_w-T_\infty)},$$

where the surface shear stress τ_w and the surface heat flux q_w are given by

$$\tau_w=\mu\left(\frac{\partial u}{\partial y}\right)_{y=0}, \quad q_w=-k^*\left(\frac{\partial T}{\partial y}\right)_{y=0},$$

Using the non-dimensional variables, one obtains

$$c_fRe_x^{1/2}=f''(0), \quad Nu_x/Re_x^{1/2}=-\theta'(0)\ \text{(VWT)}, \quad Nu_x/Re_x^{\frac{1}{2}}=\frac{1}{\theta(0)}\ \text{(VHF)}.$$

where $Re_x=\frac{U_wx}{\nu}$ is the local Reynold's number.

4. NUMERICAL SOLUTION:

The equations (8) - (11), (17) and (18) (VWT case) or (21) and (22) (VHF case) are highly nonlinear, ordinary differential equations. In order to solve these equations numerically, we follow most efficient numerical technique fourth-fifth Runge-Kutta-Fehlberg scheme with the help of Maple software, [1]. In this method, it is most important to choose a appropriate finite value of $\eta\to\infty$ (here we take $\eta=5$). The coupled boundary layer equations (8)-(11) and either in equations (17) and (18) (VWT case) or (21) and (22) (VHF case) were solved by RKF-45 method. To assess the accuracy of the numerical method used, the computed value of the skin friction co-efficient $-f''(0)$ are compared with those of (Cortell 2005) and (Chen 2009) for different values of magnetic parameter with $\beta=\alpha=Ec=Pr=f_0=N=0$. It is observed that our results are in good agreement with the results obtained by the previous investigators as seen from the tabulated results in Table 1.

Table 1: Comparison of $-f''(0)$ for various values M when $\alpha=\beta=f_0=0$.

M	Cortell [5]	Chen [4]	Present Study
0.0	1.00000	1.00000	1.00000
0.2	1.09545	1.09544	1.09544
0.5	1.22475	1.22474	1.22474
1.0	1.41421	1.41421	1.41421
1.2	1.48323	1.48324	1.48323
1.5	1.58114	1.58113	1.58113
2.0	1.73205	1.73205	1.73205

5. RESULTS AND DISCUSSION:

Consider two-dimensional, MHD boundary layer flow and heat transfer of a dusty fluid over a stretching sheet in the presence of viscous dissipation. The exact solutions do not seem feasible for a complete set of the equations (1)-(5) and (13)-(14) because of the nonlinearity and couplings between the momentum and thermal boundary layer equations. Therefore, the solutions are obtained numerically. The system of nonlinear equations (1)-(5), (13)-(14) subject to the boundary conditions (6) and (15) or (20) are converted into a system of non-linear ordinary differential equations using similarity transformations. These non-linear ordinary differential equations are then solved numerically using fourth-fifth Runge-Kutta-Fehlberg scheme with the help of Maple software. Further, velocity and temperature profiles for $\theta(\eta)$ and $\theta_p(\eta)$ in VWT case and in VHF case are depicted graphically for different values of magnetic parameter

(M), dust interaction parameter (β), Prandtl number (Pr), Eckert number (Ec) and unsteadiness parameter (α). Comparison of our results of $f''(0)$ with those obtained by Chen [3], Grubka et al. [13] and Dulal et al. [8] (see Table 2) in absence of magnetic parameter, fluid-interaction parameter, unsteady parameter, Eckert number and suction parameter. From the Tables 1 and 2, one can notice that there is a close agreement with these approaches and thus verifies the accuracy of the method used. Throughout the thermal analysis we have consider $\tau_T = \tau_v = 0.5, c_p = c_m = 0.2,\ N = 0.5, E = 0.2$ and $f_0 = 2.0$.

Table 2: Comparison of Local Nusselt number $-\theta'(0)$ for several values of Pr with $\alpha = \beta = M = f_0 = Ec = 0.0$.

M	Chen [3]	Grubka et al. [13]	Dulal et al. [8]	Present Study
0.72	1.0885	1.0885	-	1.08855
1.0	1.3333	1.3333	1.33333	1.33333
2.0			1.99999	1.99999
3.0	2.5097	2.5097	2.50971	2.50971
4.0	-	-	2.93878	2.93878
5.0	-	-	3.31647	3.31648
6.0	-	-	3.65776	3.65777
7.0	-	-	3.97150	3.97151
8.0	-	-	4.26345	4.26345
9.0	-	-	4.53760	4.53760
10.0	4.7968	4.7969	4.79687	4.79687

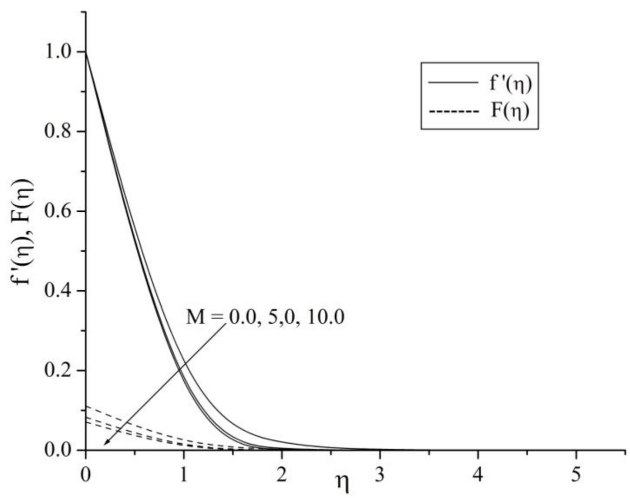

Figure 1: Effect of Magnetic parameter M on velocity profiles.

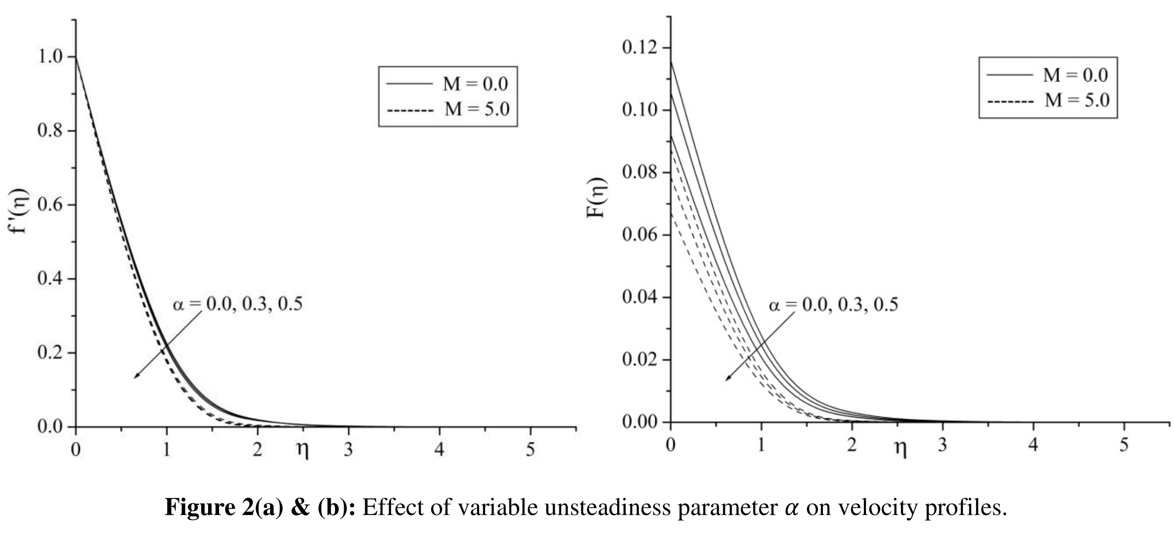

Figure 2(a) & (b): Effect of variable unsteadiness parameter α on velocity profiles.

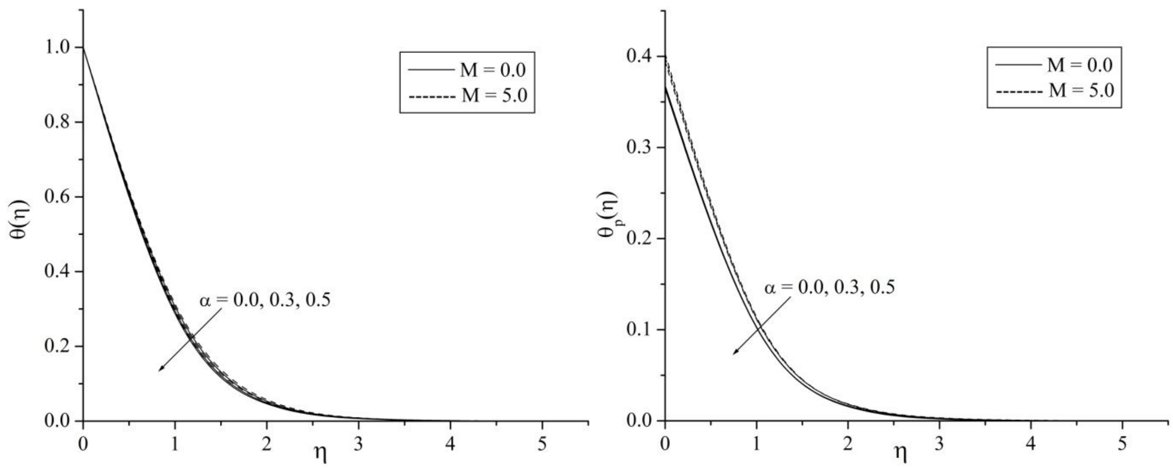

Figure 4(a): Effect of unsteadiness parameter α on temperature profiles in VWT case.

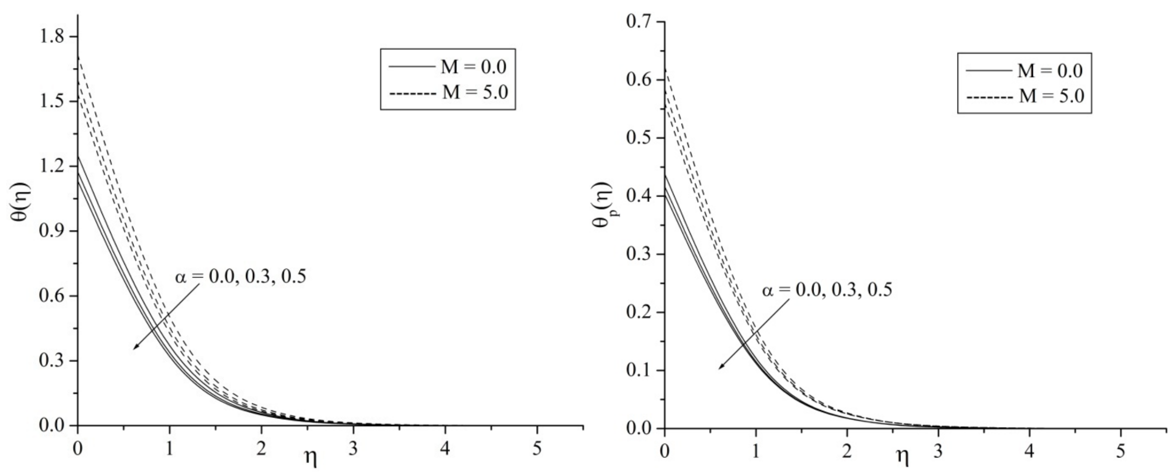

Figure 4(b): Effect of unsteadiness parameter α on temperature profiles in VHF case.

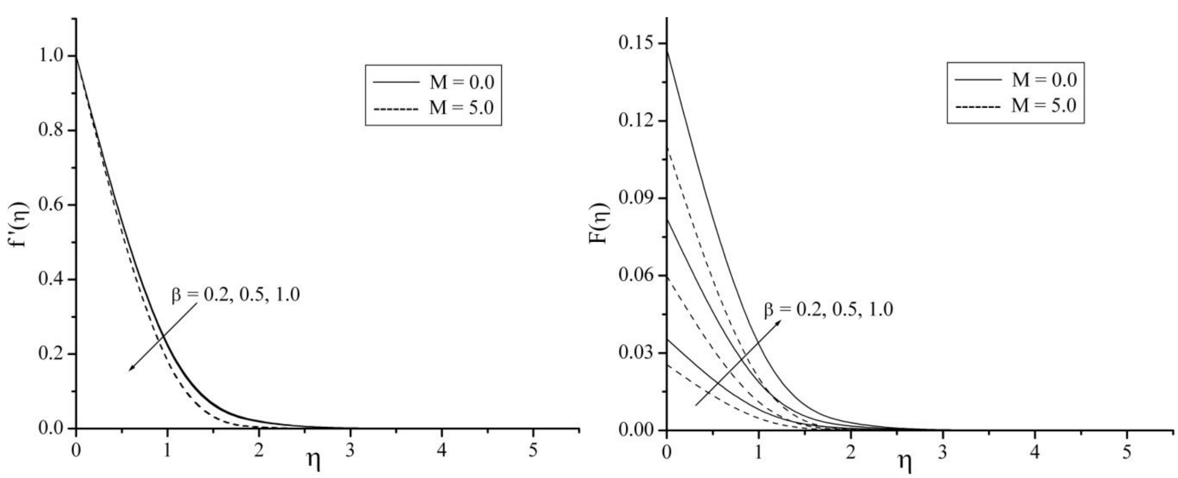

Figure 5(a) & (b): Effect of fluid-interaction parameter β on velocity profiles.

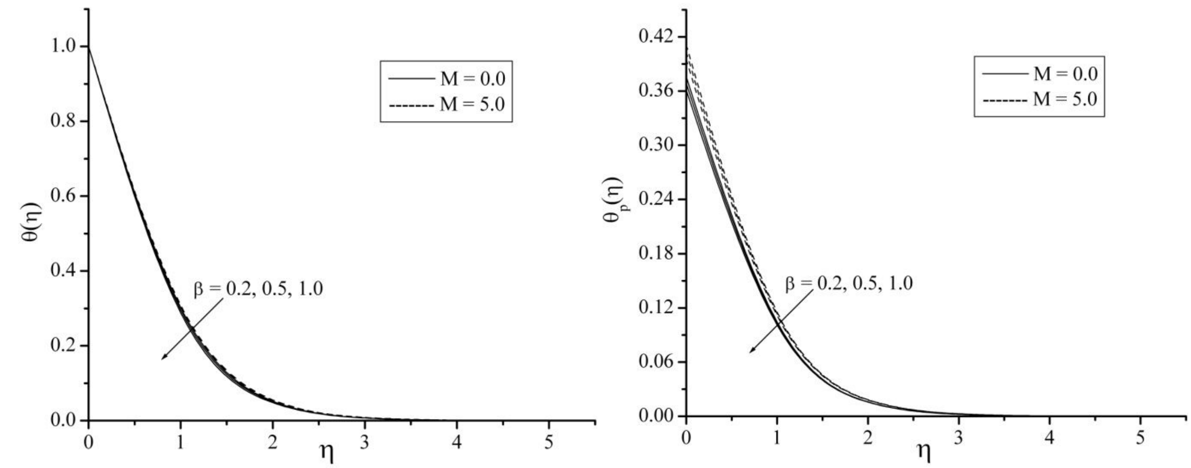

Figure 6(a): Effect of fluid-interaction parameter β on temperature profiles in VWT case.

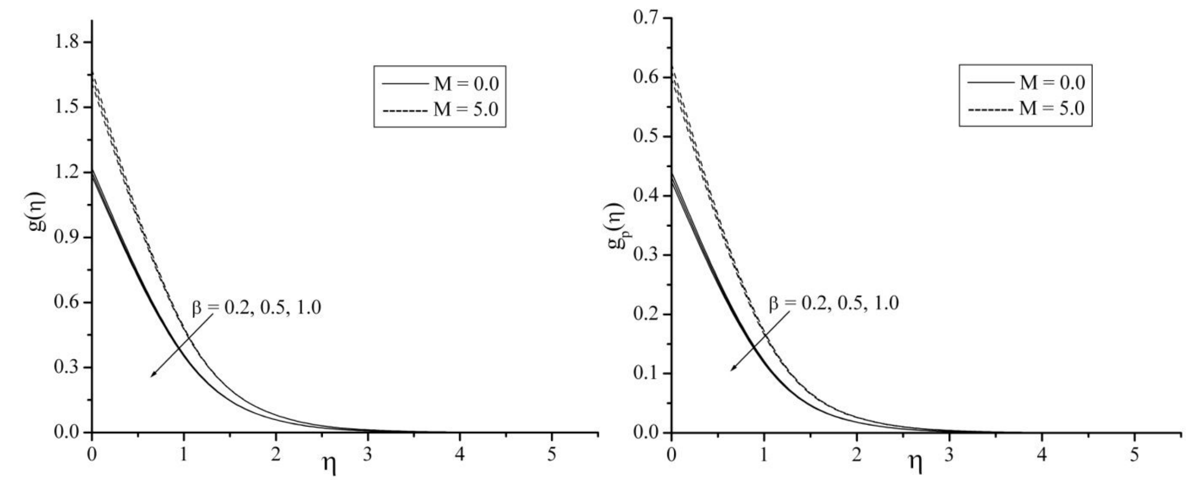

Figure 6(b): Effect of fluid-interaction parameter β on temperature profiles in VHF case.

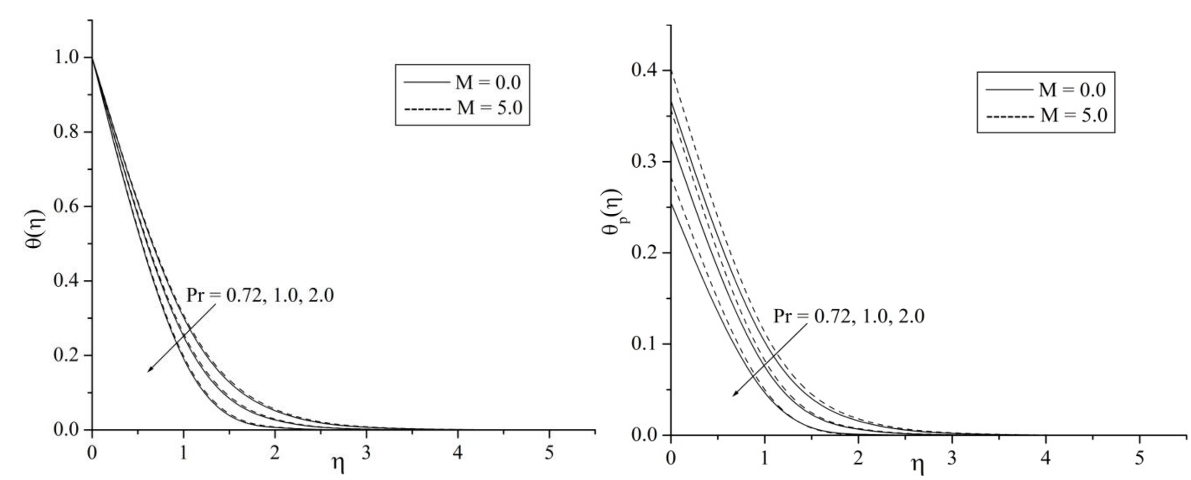

Figure 7(a): Effect of Prandtl number Pr on temperature profiles in VWT case.

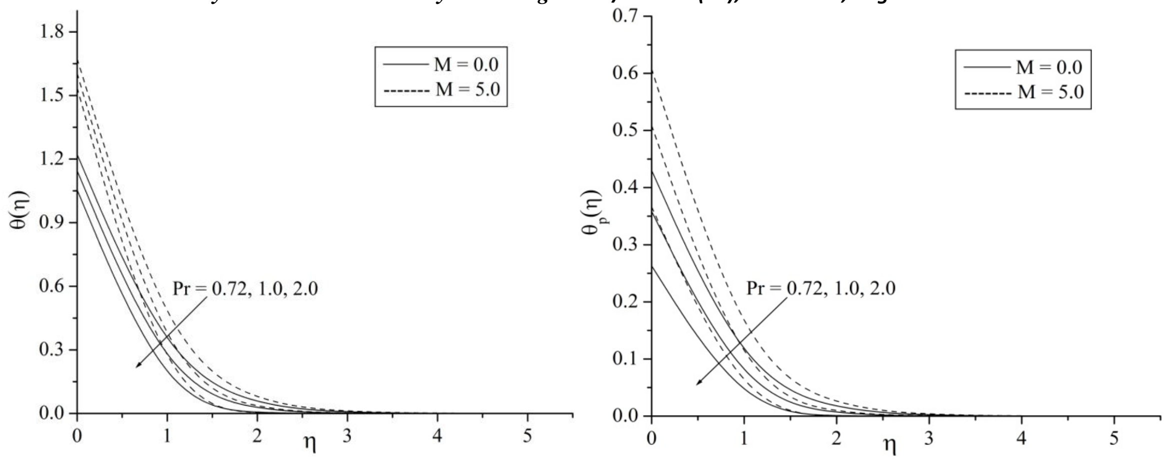

Figure 7(b): Effect of Prandtl number Pr on temperature profiles in VHF case.

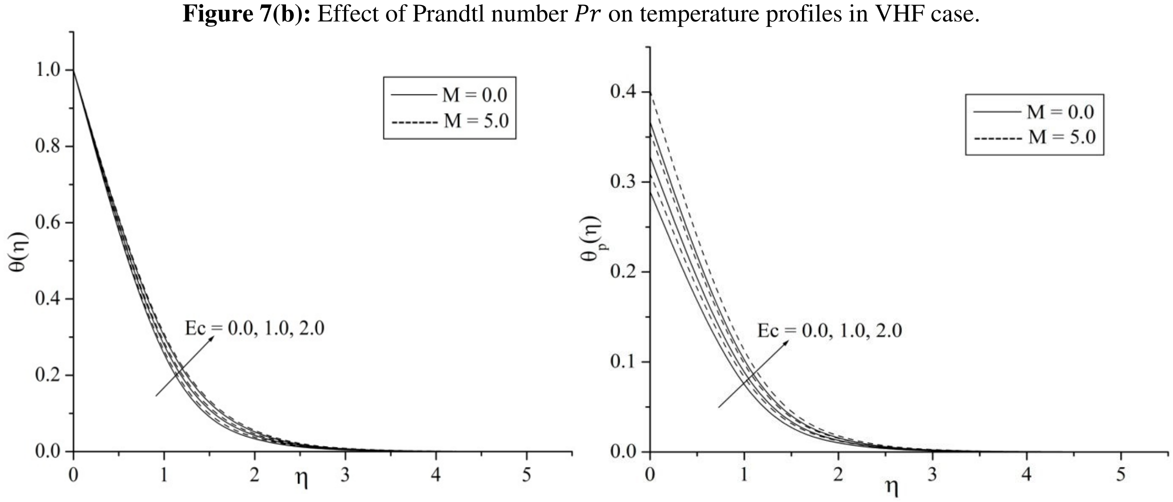

Figure 8(a): Effect of Eckert number Ec on temperature profiles in VWT case.

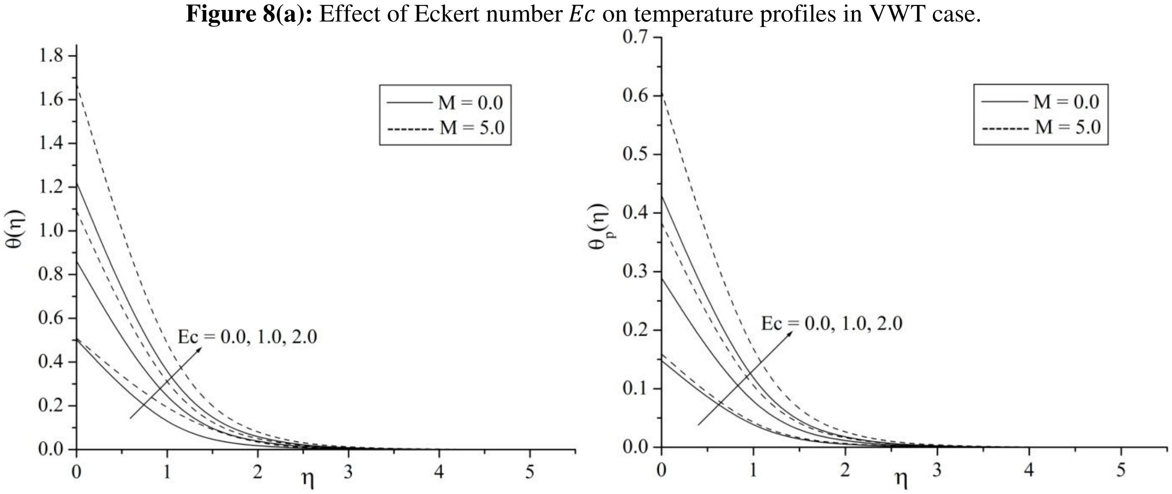

Figure 8(b): Effect of Eckert number Ec on temperature profiles in VHF case.

The dimensionless velocity profiles for fluid and dust phase for different values of magnetic parameter M with constant suction parameter are illustrated in the figure 1 when $E = 0.2, \alpha = 0.4, N = 0.5,\ \beta = 0.6,\ f_0 = 2.0$. It is clearly observed from these figures that the horizontal velocity profiles decreases with increase in η and magnetic parameter. This is due to the fact that an increase in M signifies the increase in Lorentz force, which opposes the horizontal flow. Further, it can be seen that the momentum boundary layer thickness decreases as M increases.

Figures 2(a) and 2(b), present horizontal velocity profiles for both fluid and dust phase for various values of α when $N = 0.5$. From these figures one can observed that the velocity profiles decreases with increase in the value of unsteadiness parameter. It is interesting to note that the thickness of the boundary decreases with increasing values of α.

The effect of the magnetic parameter M on the temperature profiles for fluid and dust phase in VWT and VHF cases are shown in the figures 3(a) and 3(b) with $\alpha = 0.4, \beta = 0.6, Pr = 0.72, Ec = 2.0$. By analyzing these graphs, one can see that the effect of increasing values of M increases the temperature distributions in the boundary layer in both VWT and VHF cases. This is because of the fact that the introduction of transverse magnetic field to an electrically conducting fluid gives rise to a resistive force, known as Lorentz force. This force has a tendency to slow down the motion of the fluid in the boundary layer and to increase the temperature distribution.

Figure 4(a) and 4(b) shows the temperature profiles for different values of unsteadiness parameter α for VWT and VHF cases ($\beta = 0.6, Pr = 0.72, Ec = 2.0$) respectively. It is observed from these figures that the temperature profiles decreases smoothly with η in the absence of unsteadiness parameter ($\alpha = 0.0$) whereas the temperature profiles continuously decreases with increase in α. This shows an important fact that the rate of cooling is much faster for higher values of unsteadiness parameter whereas it may take longer time for cooling during steady flows.

It is evident from the figure 5(a) and 5(b) that the flow is parabolic in nature and we can see that the flow of fluid particles is parallel to that of dust. Further observation shows the effect of fluid particle interaction parameter β on velocity components of the fluid velocity $f'(\eta)$ and particle velocity $F(\eta)$ i.e. if β increases we can find the decrease in the fluid phase velocity and increase in the dust phase velocity. Also it reveals that for the large values of β i.e. the relaxation time of the dust particles decreases then the velocities of both fluid and dust particles will be the same.

Figures 6(a) and 6(b) are graphical representation for the temperature distributions for VWT and VHF case, for different values of β versus η with $Pr = 0.72, \alpha = 0.1, Ec = 2.0$. We infer from these figures that temperature of the fluid and dust particle decreases with increases in β respectively.

Figures 7(a) and 7(b) depict the temperature profiles $\theta(\eta)$ and $\theta_p(\eta)$ versus η from the sheet for both VWT and VHF cases on different values of Pr with $\beta = 0.6, \alpha = 0.1, Ec = 2.0$. We figures that temperature decreases with increases in Pr which implies viscous boundary layer is thicker than the thermal boundary layer. The increase of Prandtl number means that the slow rate of thermal diffusion. However, the effect of increasing value of Prandtl number increases temperature distributions near the boundary and decreases everywhere away from the boundary in VWT case. However, it may be other than the unity in VHF case due to adiabatic temperature boundary condition.

The figures 8(a) and 8(b) shows the temperature distributions $\theta(\eta)$ and $\theta_p(\eta)$ versusη from the sheet, for different values of Eckert number Ec in both VWT and VHF cases, respectively when $\beta = 0.6, \alpha = 0.1, Pr = 0.72$. By analyzing the graphs it reveals that the effect of increasing values of Ec increases the temperature distributions in flow region in both VWT and VHF cases. This is due to the fact that heat energy is stored in the liquid due to the frictional heating. The effect of increasing Ec enhanced the temperature at any point and this is true in both cases. Further one can notice that the combined effect of suction parameter V_w and increasing values of Eckert number Ec reduces the temperature distribution significantly.

Table 3: Values of wall temperature gradient $\theta'(0)$ (for VWT Case) and wall temperature $\theta(0)$ (for VHF Case) with $E = 0.2, N = 0.5, f0 = 2.0$.

α	β	M	Pr	Ec	$\theta'(0)(VWT)$	$\theta(0)(VHF)$
0.0	0.6	3.0	0.72	2.0	0.168325	1.556538
0.2					0.063300	1.486246
0.4					-0.033995	1.425695
0.2	0.0	3.0	0.72	2.0	0.068473	1.489875
	0.3				0.064501	1.487212
	0.6				0.063300	1.486246
0.2	0.6	0.0	0.72	2.0	-0.557699	1.197127
		3.0			0.063300	1.486246
		5.0			0.373055	1.634765
0.2	0.6	3.0	0.72	2.0	0.063300	1.486246
			1.00		0.211231	1.421561
			2.00		0.830031	1.354481
0.2	0.6	3.0	0.72	0.0	-2.102027	0.496043
				0.5	-1.560695	0.743594
				1.0	-1.019363	0.991145

6. CONCLUSIONS:

The two-dimensional boundary layer flow and heat transfer of an unsteady dusty fluid over a stretching sheet is considered. Viscous dissipation is included in the energy equation. The governing partial differential equations are reduced into set of non-linear ordinary differential equations using the suitable similarity transformations. The coupled non-linear ordinary differential equations are solved numerically by applying RKF-45 order method using Maple software. Temperature profiles are obtained for two types of heating processes namely, VWT and VHF for various values of physical parameters. The effects of magnetic parameter, Prandtl number, Eckert number and unsteadiness parameter on the dynamics are presented graphically in Figs.1-8. Further, the values of thermal heat characteristics at the wall temperature gradient function $\theta'(0)$ (VWT) and wall temperature $\theta(0)$ (VHF) are tabulated in the Table 3. The major findings from the present study can be summarized as follows:

1. Boundary layer flow attains minimum velocity for higher values of magnetic parameter M.
2. The thickness of the momentum boundary layer decreases with increase in the magnetic parameter and unsteadiness parameter in velocity profiles.
3. Fluid phase temperature is higher than the dust phase temperature.
4. The effect of viscous dissipation increases the temperature in the boundary layer region.
5. The effect of increasing the values of Prandtl number Pr increases temperature largely near the stretching sheet for both VWT and VHF cases.
6. The increasing value of the Prandtl number reduces both the temperature distribution and heat transfer rate.
7. The temperature profile increases with increase in the Eckert number.
8. If $\beta \to 0, \alpha \to 0$ then our results coincides with the results of Cortell [5] and Chen [4] when magnetic number varies.
9. If $\beta \to 0, \alpha \to 0, Ec \to 0$ and $N \to 0$ then our results coincides with the results of Chen [3], Grubka et al. [13] and Dulal et al. [8] when Prandtl number varies.

ACKNOWLEDGEMENT:

We wish to express our thanks to DST (Department of Science and Technology), New Delhi for financial support to pursue this work under a Major Research Project (Grant no: SR/S4/MS: 470/07, 25-08-2008).

REFERENCES:

1. Abdul Aziz, *A similarity solution for laminar thermal boundary layer over a flat plate with a convective surface boundary condition*, Com. Non. Sci. Num. Simul., **14** (2009) 1064-1068.

2. S.P.Anjali Devi and B.Ganga, *Dissipation effects on MHD nonlinear flow and heat transfer past a porous surface with prescribed heat flux*, J. of Appl. Fluid Mech., **3**(1) (2010) 1-6.

3. C.H.Chen, *Laminar mixed convection adjacent to vertical continuously stretching sheets*, Heat and Mass Transfer, **33** (1998) 471-476.

4. C.H.Chen, *Magneto-hydrodynamic mixed convection of a power-law fluid past a stretching surface in the presence of thermal radiation and internal heat generation/absorption* Int. J. Non-linear Mech., **44** (2009) 596-603.

5. R.Cortell, *A note on magnetoyhdrodynamic flow of a power-law fluid over a stretching sheet*, Appl. Math. Comput., **168**(1) (2005) 557-566.

6. L.J.Crane, *Flow past a stretching plate*, Z. Angew. Math. Phy., **21**(4) (1970) 645-647.

7. N.Datta and S.K.Mishra, *Boundary layer flow of a dusty fluid over a semi-infinite flat plate*, Acta Mechanica, **42**(1-2) (1982) 71-83.

8. Dulal Pal and Hiranmoy Mondal, *Hydromagnetic non-Darcy flow and heat transfer over a stretching sheet in the presence of thermal radiation and Ohmic dissipation*, Com. Non. Sci. Num. Simul., **15**(5) (2010) 1197-1209.

9. E.M.A.Elbashbeshy and M.A.A.Bazid, *Heat transfer over an unsteady stretching surface*, Heat and Mass Transfer, **41**(1) (2004) 1-4.

10. B.J.Gireesha, S.Manjunatha and C.S.Bagewadi, *Unsteady hydromagnetic boundary layer flow and heat transfer of dusty fluid over a stretching sheet*, Afrika Metametika (Springer) **22** (2011) (Article in Press).

11. B.J.Gireesha, G.K.Ramesh, M.Subhas Abel and C.S.Bagewadi, *Boundary layer flow and heat transfer of a dusty fluid flow over a stretching sheet with non-uniform heat source/sink*, Int. J. of Multiphase Flow, **37**(8) (2011) 977-982.

12. B.J.Gireesha, G.S.Roopa and C.S.Bagewadi, *Boundary layer flow of an unsteady dusty fluid and heat transfer over a stretching sheet with non-uniform heat source/sink*, Engineering (Scientific Research), **3**(7) (2011) 726-735.

13. L.J.Grubka and K.M.Bobba, *Heat transfer characteristics of a continuous, stretching surface with variable temperature*, Int. J. of Heat and Mass Transfer, **107**(1) (1985) 248-250.

14. B.C.Sakiadis, *Boundary layer behavior on continuous solid surfaces: I. Boundary layer equations for two dimensional and axisymmetric Flow*, AIChE Journal, **7**(1) (1961) 26-28.

15. B. C. Sakiadis, Boundary layer behavior on continuous solid surfaces: II. Boundary layer on a continuous flat surface, AIChE Journal, **7**(2) (1961) 221-225.

16. H.Schlichting, Boundary layer theory, McGraw-Hill, (1968).

17. S.Sharidan, T.Mahmood and I.Pop, *Similarity solutions for the unsteady boundary layer flow and heat transfer due to a stretching sheet*, Int. J. of Appl. Mech. Eng., **11**(3) (2006) 647-654.

18. K.Vajravelu and A.Hadjinicolaou, *Heat transfer in a viscous fluid over a stretching sheet with viscous dissipation and internal heat generation*, Int. Comm. Heat Mass Transfer, **20**(3) (1993) 417-430.

19. K.Vajravelu And J.Nayfeh, *Hydromagnetic flow of a dusty fluid over a stretching sheet*, Int. J. Non-linear Mech., **27**(6) (1992) 937-945.

20. P.H.Veena, Subhash Abel, K.Rajagopal and V.K.Pravin, Heat transfer in a visco-elastic fluid past a stretching sheet with viscous dissipation and internal heat generation, Z. angew. Math. Phys., **57**(3) (2006) 447-463.

****

